

## Fenton-like catalytic oxidation of Reactive Red 195 by FeNi<sub>3</sub>/SiO<sub>2</sub>@H<sub>2</sub>O<sub>2</sub>: adsorption and degradation study

Anis Ahmadi<sup>a</sup>, Behnam Barikbin<sup>b,c</sup>, Maryam Khodadadi<sup>b,\*</sup>

<sup>a</sup>Student Research Committee, Faculty of Health, Birjand University of Medical Sciences, Birjand, Iran, email: ahmadi9014@gmail.com

<sup>b</sup>Social Determinants of Health Research Center, Birjand University of Medical Sciences, Birjand, Iran, emails: maryam.khodadadi@gmail.com (M. Khodadadi), b\_barikbin@yahoo.com (B. Barikbin)

<sup>c</sup>Social Determinants of Health Research Center, Mashhad University of Medical Sciences, Mashhad, Iran

Received 19 February 2020; Accepted 2 January 2021

### ABSTRACT

Dyes are among the superlative hazardous chemical compounds in industrial wastewater, including textile wastewater. The aim of this study was magnetic nanocomposite FeNi<sub>3</sub>/SiO<sub>2</sub> synthesis and review its efficiency in the removal of Reactive Red 195 (RR195) from the aqueous solutions. In the present research, the effects of important variables such as the initial concentration of pH (3, 5, 7, 9, and 11), contact time (5, 10, 15, 30, 60, 90, 120, and 180 min), dye concentration (5, 10, 20, 30, and 40 mg/L), nanocomposite dose (1, 2, 4, and 6 g/L), and H<sub>2</sub>O<sub>2</sub> concentration (50, 100, 150, and 200 mg/L) on the removal of Reactive Red 195 dye were investigated. The synthesized nanocomposite specification was also studied using Brunauer–Emmet–Teller, Fourier transform infrared, field emission scanning electron microscopy, and vibrating sample magnetometer techniques. The results of the study showed that increasing the contact time and reducing the dye concentration, increased the removal efficiency, so that the highest removal percentage of Reactive Red 195 was 100% at pH = 3, with dye concentration of 5 mg/L, FeNi<sub>3</sub>/SiO<sub>2</sub> dosage of 1 g/L, and H<sub>2</sub>O<sub>2</sub> dosage of 100 mg/L in contact time 90 min. Diagnostic techniques also confirmed the synthesis of synthesized nanocomposite with appropriate quality. According to the results, the Fenton-like catalytic process of FeNi<sub>3</sub>/SiO<sub>2</sub>@H<sub>2</sub>O<sub>2</sub> had high performance in removing Reactive Red 195 dye from aqueous solutions. It could be concluded that this method can effectively be used in the treatment of colored sewage.

*Keywords:* Reactive Red 195; FeNi<sub>3</sub>/SiO<sub>2</sub>; Removal; Fenton-like; Aqueous solutions

### 1. Introduction

Colors are almost dangerous chemicals in industrial wastewater and they are highly utilized in many various industries such as food, medicine, textile, knitting, plastics, cosmetics, leather, and paper industries [1]. Nevertheless, in terms of color making, the more significant industries are usually the textile and coloring industries [2]. The textile industry plays an important role of industries in developing countries [3]. About one-fifth of total paint production in the textile industry goes into the environment through sewage [4].

Colors are divided into three main classes: anionic (direct, acidic, and reactive), cationic (all basic colors), and non-ionic (dispersed colors) [5]. Azoic dyes are the largest group of dyes used for textile dyeing and other industrial applications [6].

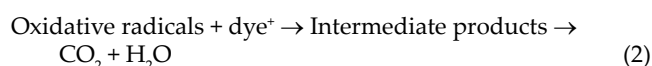
Dyes are chemical compounds that are of great importance for a number of reasons, including reducing the permeability of light and subsequently disrupting the process of photosynthesis in water sources. Aesthetically, these compounds also have a negative effect on water quality and lead to sensitivity, dermatitis, cancer, and genetic mutations in humans [7]. The toxic effects of dyes can be

\* Corresponding author.

passed on to future generations in the form of genetic mutations, birth defects, and hereditary diseases [5]. Reactive Red 195 contains an active group consisting of an aromatic heterocyclic ring containing fluoride or chloride ions [8]. It is commonly used to dye cellulose fabrics and to print on fabric tissue [9]. Dye containing wastewater usually has high chemical oxygen demand (COD), total dissolved solids (TDS), and high dye content and low biodegradability [10]. Different physical, chemical, and biological procedures have been used to omit dyes of aqueous solutions [4]. Conventional physical and chemical treatment methods such as flocculation, chemical precipitation, adsorption, buoyancy, and membrane processes (ultrafiltration, reverse osmosis) have not been able to degrade these compounds and can only absorb and transfer them from one phase to another and lead to secondary environmental pollution [11]. Although these methods have been proven to be efficient, they have constraints such as excessive use of chemicals or cumulating of sludge, high operating expense, lack of effectual color decrement, and sensibility to incoming sewage changes [12]. One of the most important methods for removing dyes from polluted wastewater is advanced oxidation processes (AOPs) [13]. The Fenton is one of the advanced oxidation procedures. The Fenton method, which is divided into Fenton-like, electro-Fenton, photo-Fenton, and dark-Fenton types uses reagents that are readily available, inexpensive, and environmentally safe [14,15].

In addition, recently, nanotechnology has been widely used for water and wastewater treatment [16]. The main advantage of nanotechnology is its capacity to purify large amounts of wastewater in a short time and produce less pollution [17]. The reason for the use of nanomaterials (NMS) such as nano-sized metal oxides as catalysts in industrial wastewater treatment plants is due to their high activity [18]. One of the benefits of magnetic nanoparticle-based catalyst systems is that they provide a wide surface area for reactive molecules and are easily detachable and reusable upon completion of the reaction [16].

The following reactions occur when using heterogeneous Fenton-like oxidation for de-colorization: initially, oxidizing radicals ( $\text{HO}_2^{\cdot}$  and  $\text{OH}^{\cdot}$ ) are formed that react with color molecules and mediate the production of products, followed by the mineralization process ( $\text{CO}_2 + \text{H}_2\text{O}$ ), shown in Eqs. (1) and (2):



The dye de-colorization is caused by the breakdown of the N bond by adding  $\text{OH}^{\cdot}$  radical. The oxidation of intermediate products of  $\text{H}_2\text{O}$  and  $\text{CO}_2$  causes the mineralization of color, which is slower than dye omission due to  $\text{OH}^{\cdot}$  attack on N=N bands [19,20].

For example, photocatalytic degradation of tetracycline was performed by magnetic nanocomposite  $\text{FeNi}_3/\text{SiO}_2/\text{CuS}$  [16] as well as magnetic nanocomposite  $\text{FeNi}_3@\text{SiO}_2@\text{TiO}_2$  [21] as well as tamoxifen degradation using  $\text{FeNi}_3@\text{SiO}_2@\text{ZnO}$  [22]. In recent years, other catalytic degradations

such as heterogeneous electro-Fenton treatment and electrochemical treatment were used to degrade Reactive Red 195 dye [23,24]. Therefore, given the negative effects that reactive dyes may have on the environment, the use of magnetic nanocomposites, and Fenton-like catalytic processes are among the new approaches in water and wastewater treatment. Therefore, the aim of present study was to survey the efficiency of  $\text{FeNi}_3/\text{SiO}_2$  magnetic nanocomposites separately and in combination with  $\text{H}_2\text{O}_2$  in Fenton-like catalytic process ( $\text{FeNi}_3/\text{SiO}_2@\text{H}_2\text{O}_2$ ) for Reactive Red 195 removal from aqueous solutions.

## 2. Materials and methods

### 2.1. Materials and devices

The dye used in this study was Reactive Red 195 (RR195) dye, with a molecular weight of 1,136.32 and its molecular formula  $\text{C}_{31}\text{H}_{19}\text{ClN}_7\text{Na}_3\text{O}_{19}\text{S}_6$ . The chemical structure is shown in Fig. 1 [17]. The UK's PG spectrophotometer (spectrometer T80<sup>+</sup> with a wavelength of 540 nm) was used to measure the residual dye concentration [9]. The UV/vis UK spectrophotometer (spectrometer T80<sup>+</sup> model with the wavelength of 540 nm) was used to measure residual color concentration [9].

Other materials used include: hydrazine hydrate of formula  $\text{N}_2\text{H}_4\cdot\text{H}_2\text{O}$  with 80% purity, ethanol ( $\text{C}_2\text{H}_5\text{OH}$ ), tetraethyl ortho silicate (TEOS) with formula  $\text{SiC}_8\text{H}_{20}\text{O}_4$ ,  $\text{FeCl}_2(4\text{H}_2\text{O})$ , hydrogen peroxide 30%, polyethylene glycol (1 g MW 600),  $\text{NiCl}_2\cdot(6\text{H}_2\text{O})$ , HCl, and NaOH that were all Merck company products (Germany). Dionysian water was used to make the solutions. The method described in Standard Method book no. 5220 was used to measure COD [25].

Devices used include a spectrophotometer (UV/vis T80<sup>+</sup> model), Fourier transform infrared (FTIR; US AVATAR 370 model with spectrometer in the range 400–4,000  $\text{cm}^{-1}$ ), field emission scanning electron microscopy (FESEM; SLGMA Vp-500 Zeiss model made in Germany), and vibrating sample magnetometer (VSM; LAKE shore 7404 model made in the USA).

### 2.2. Synthesis of $\text{FeNi}_3/\text{SiO}_2$ nanocomposite

The synthesis was performed as follows:

For the synthesis of  $\text{FeNi}_3$ , the amount of 1 g polyethylene glycol 6000 in 180 mL of deionized water was dissolved. Then, in 30 mL of water deionized amount 0.71 g of nickel chloride and 0.198 g of iron chloride solution were added separately to the initial solution. After complete mixing, the pH of the solution was adjusted from 12 to 13 using sodium hydroxide. Finally, 9.1 mL of hydrazine hydrate ( $\text{N}_2\text{H}_4\cdot\text{H}_2\text{O}$ ) was added to the obtained suspension at 80% concentration. The reaction was carried out at ambient temperature for 24 h and during this time the pH was constantly monitored to maintain the desired range [26].

After the synthesis of  $\text{FeNi}_3$ , the magnetic  $\text{FeNi}_3$  was core-shelled with  $\text{SiO}_2$ . For this purpose, 0.5 g of magnetic nanoparticles of  $\text{FeNi}_3$  was synthesized in a mixture containing 80 mL of ethanol, 20 mL of deionized water, and 2 mL of 28% ammonia. Then, 1 mL of TEOS was added dropwise to the available solution and stirred at 500 rpm for 24 h at environment temperature. Eventually, the obtained

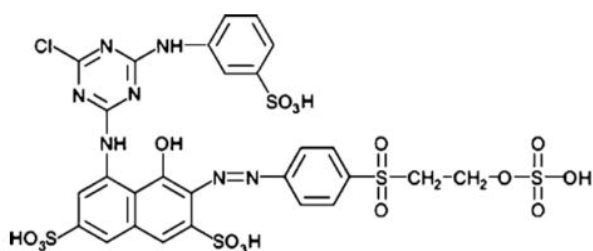


Fig. 1. Chemical structure of Reactive Red 195.

magnetic  $\text{FeNi}_3/\text{SiO}_2$  nanocomposites were washed several times with water and ethanol. The nanocomposite was dried at  $60^\circ\text{C}$  in a vacuum oven after being separated by an exterior magnetic field [27]. After synthesizing the nanocomposite, it was characterized using VSM, FTIR, FESEM, and Brunauer–Emmet–Teller (BET) diagnostic techniques.

### 2.3. Reactive Red 195 dye adsorption and removal experiments

Reactive Red 195 dye adsorption experiments in the presence of  $\text{FeNi}_3/\text{SiO}_2$  and dye removal in the Fenton-like catalytic process using  $\text{FeNi}_3/\text{SiO}_2@H_2O_2$  were carried out as follows:

The stock solution of 1,000 mg/L of Reactive Red 195 dye was made and was used to make other solutions at different concentrations. pH set up was done by 0.1 M HCl and NaOH solution. Then, by adding a specific dose of adsorbent to the sample containing a certain concentration of Reactive Red 195 dye, the sample was stirred on the shaker for a specific time.

The variables studied in the removal and adsorption phase were contact time (5, 10, 15, 30, 60, 90, 120, and 180 min), the initial pH of the solution (3, 5, 7, 9, and 11), adsorbent dose (1, 2, 4, and 6 g/L), initial concentration of Reactive Red 195 dye (5, 10, 20, 30, and 40 mg/L), and  $H_2O_2$  concentration (50, 100, 150, and 200 mg/L). The equilibrium adsorption capacity of the synthesis adsorbent was calculated by Eq. (3).

$$q_e = \frac{(C_0 - C_e) \times V}{M} \quad (3)$$

In this Eq. (3),  $q_e$  is the value of ions adsorbed per unit mass of adsorbent,  $C_0$  is the initial concentration of metal ions in solution in mg/L,  $C_e$  is the equilibrium concentration of metal ions in solution in mg/L,  $V$  is sample volume per liter, and  $M$  is adsorbent weight in g. Adsorption performance and adsorbent ability to adsorb ions from aqueous solution were evaluated by Langmuir and Freundlich isotherm models. The Langmuir model proposes that the adsorption in a single layer or in a fixed number of adsorption sites on the surface all have equal energy adsorption sites, assuming that the adsorbent structure is homogeneous. The Langmuir equation is expressed in Eq. (4):

$$\frac{C_e}{q_e} = \frac{1}{q_{\max} k_L} + \left( \frac{C_e}{q_{\max}} \right) \quad (4)$$

In Eq. (4),  $q_e$  is the balance ions of the metal are absorbed in mg/g,  $q_m$  is the maximum adsorption capacity in mg/kg, the balanced concentration of the metal ion in solution is expressed in mg/L, Langmuir constant  $k_L$  denotes Langmuir adsorption equilibrium constant in 1/mg, the Freundlich isotherm model describes the adsorption in a heterogeneous system. This model is given by Eq. (5):

$$q_e = K_F C_e^{1/n} \quad (5)$$

In Eq. (5),  $q_e$  is the value of equilibrium ions adsorbed on the metal in mg/g, the  $C_e$  is balanced concentration of the metal ion in the solution in mg/L, the Freundlich constant  $K_F$ , and the determinant of the adsorbent capacity and  $n$  Freundlich is the power, that expresses the hardness or intensity of the adsorption. Eq. (6) was used to calculate the removal efficiency, where  $C_0$  and  $C_F$  (mg/L) were the initial and final concentrations of Reactive Red 195 dye, respectively:

$$\%R = \frac{(C_0 - C_F)}{C_0} \times 100 \quad (6)$$

To investigate the rate of catalytic Fenton-like removal process ( $\text{FeNi}_3/\text{SiO}_2@H_2O_2$ ), the velocity kinetic was calculated using pseudo-first-order (PFO) model and Hinshelwood equation (L–H) Eq. (7):

$$\ln \frac{C}{C_0} = -K_{\text{obs}} t \quad (7)$$

where  $K_{\text{obs}}$  is the constant of the reaction rate (PFO) in terms of ( $\text{min}^{-1}$ ),  $t$  is the reaction time (min),  $C$  is the concentration remaining after reaction (mg/L), and  $C_0$  is the initial concentration in (mg/L).

## 3. Results and discussion

In order to investigate the chemical structure of  $\text{FeNi}_3/\text{SiO}_2$  synthesized magnetic nanocomposite, FTIR technique based on the vibration of metal bonds was used. Fig. 2a demonstrates absorption bands of peaks at 479; 669; 804 (various metal bonds); 972; and  $1,124 \text{ cm}^{-1}$  which is indicated of Fe–Ni, Ni–Fe–Ni, Fe–Ni–Ni, and Si–O–Si functional group bonds, respectively [28].

To scrutinize the magnetic attributes of synthesized  $\text{FeNi}_3/\text{SiO}_2$  magnetic nanocomposites, vibration of sample (VSM) was studied at room temperature. Fig. 2b showed that in the first step, the synthesized  $\text{FeNi}_3$  nanoparticle had a magnetic property of 79.07 emu/g and in the next step of synthesis ( $\text{FeNi}_3/\text{SiO}_2$ ) its magnetic intensity decreased to 51.87 emu/g. The synthesized adsorbent is dispersed and can be dispersed again. These particles also had good magnetic properties, indicating the potential application of magnetic adsorbents that can be easily detached using an external magnet.

To study morphology and magnetic properties of  $\text{FeNi}_3/\text{SiO}_2$  magnetic nanocomposite and its size, FESEM technique was used, as shown in Fig. 2c. The size of the synthesized nanoparticles was 37.16–84 nm, indicating that the size of the nanoparticles was appropriate [29].

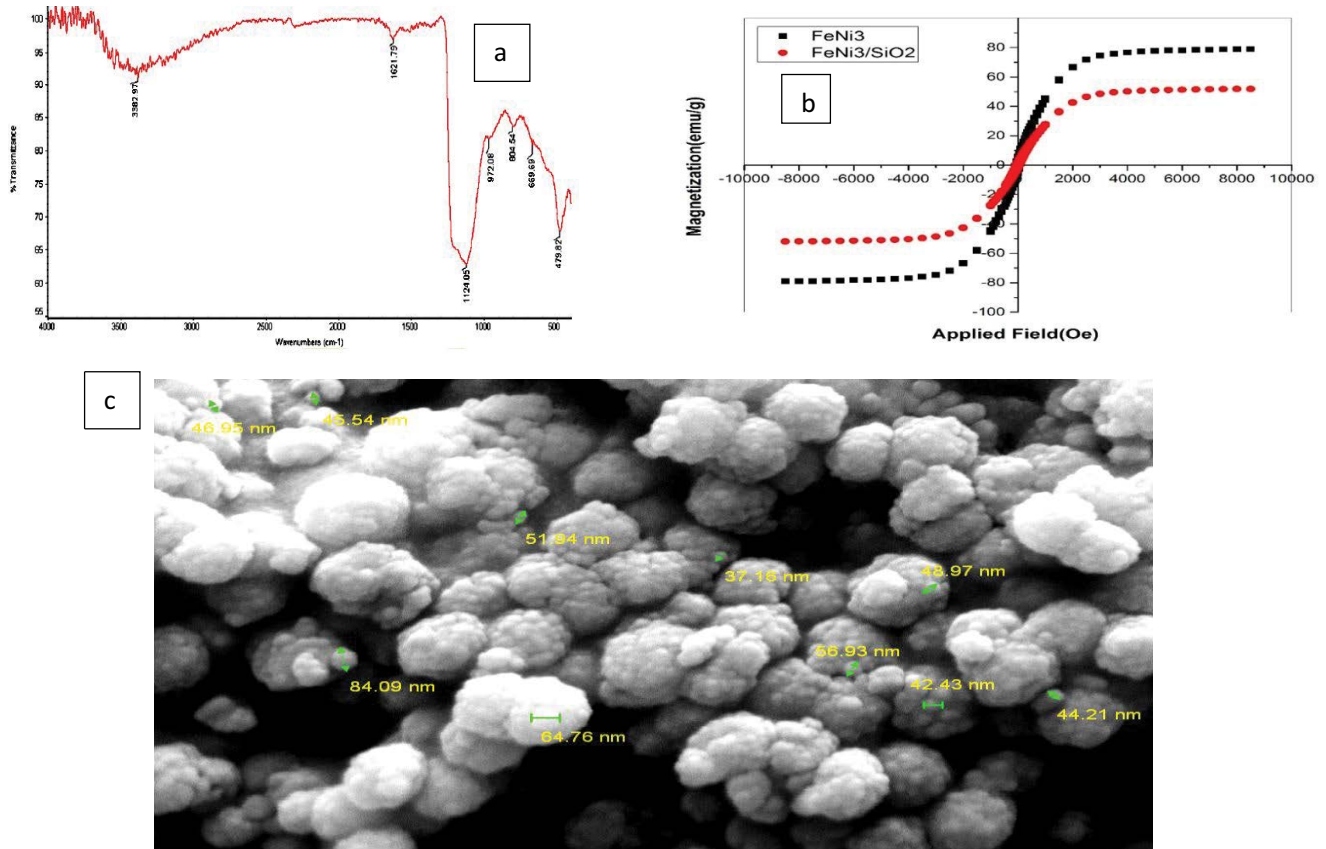


Fig. 2. (a) FTIR, (b) VSM, and (c) FESEM spectrum of  $\text{FeNi}_3/\text{SiO}_2$  magnetic nanocomposite.

BET analysis was also used to measure the porosity and effective surface area of  $\text{FeNi}_3/\text{SiO}_2$  nanocomposite with an effective surface area of  $418 \text{ m}^2/\text{g}$ .

### 3.1. Reactive Red 195 dye adsorption and removal process

#### 3.1.1. Reactive Red 195 dye adsorption process using $\text{FeNi}_3/\text{SiO}_2$

To investigate the adsorption process by  $\text{FeNi}_3/\text{SiO}_2$  magnetic nanocomposite, batch adsorption experiments under the influence of studied variables such as: pH (3–11), adsorbent dose (1, 2, 4, and 6 g/L), contact time (5–180 min), and dye concentration (5–40 mg/L) were conducted. The results showed that the highest percentage of adsorption was achieved at pH = 3 at 85% which decreased with increasing pH of adsorption efficiency, meaning that by increasing pH from 3 to 11 the removal reduced from 85% to 65%.

On the removal of Reactive Red 195 dye from aqueous solutions by  $\text{TiO}_2$  nanoparticles, the results showed that the highest rate of dye removal at pH = 3 was about 100%, and removal efficiency decreased with increasing pH [30]. This is in line with the results showed by Belessi et al. [30].

On the adsorption and photocatalysis of  $\text{TiO}_2$  nanocrystalline particles to remove Reactive Red 195, the results also showed that dye adsorption efficiency decreased with

increasing pH [4], which is in conformity with the study of Chladkova et al. [4]. In addition, the  $\text{pH}_{\text{ZPC}}$  of the  $\text{FeNi}_3/\text{SiO}_2$  magnetic nanocomposite was 7.5. At  $\text{pH}_{\text{ZPC}}$  under  $\text{pH}_{\text{ZPC}}$  the surface charge of the nanocomposite is positive and at pHs above that, the surface charge is negative and since the Reactive Red 195 dye is an anionic compound, it is better absorbed in the acidic environment [31].

The initial concentration of Reactive Red 195 dye is effective in its absorption rate by  $\text{FeNi}_3/\text{SiO}_2$  magnetic nanocomposite and as shown in Fig. 3, the removal efficiency decreased with increasing dye concentration. At the initial concentration of 5 mg/L, the removal percentage was 98% but at 40 mg/L, the removal percentage decreased to 79%.

Experimental study of the effect of adsorbent dose on the  $\text{FeNi}_3/\text{SiO}_2$  magnetic nanocomposite absorption process of Reactive Red 195 showed that the highest absorption rate was (99.6%) at 4 g/L nanocomposite dose.

The isotherm and kinetics of the Reactive Red 195 dye adsorption by  $\text{FeNi}_3/\text{SiO}_2$  were also investigated. Table 1 shows the results of the isotherm parameters for  $\text{FeNi}_3/\text{SiO}_2$  Reactive Red 195. The study of Freundlich and Langmuir isotherms revealed that the Reactive Red 195 adsorptions fitted with the Langmuir isotherm with a correlation coefficient of  $R^2 = 0.999$  as is shown in Table 1 (Fig. 4).

Table 2 shows the kinetics parameters of Reactive Red 195 dye absorption by  $\text{FeNi}_3/\text{SiO}_2$ . The pseudo-first-order

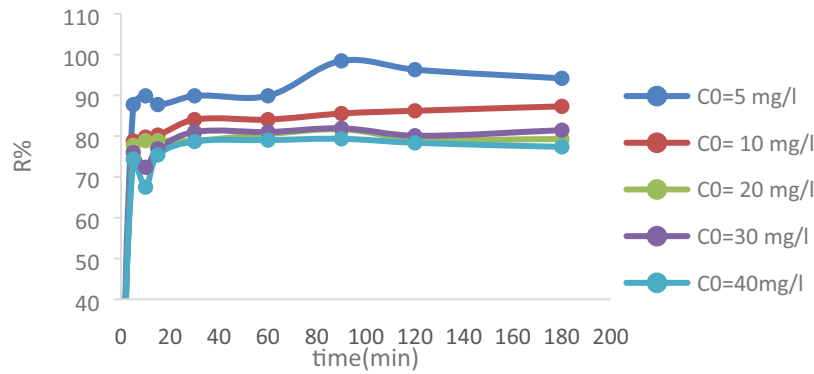


Fig. 3. Effect of initial soluble concentration on the adsorption rate of Reactive Red 195 at different times by FeNi<sub>3</sub>/SiO<sub>2</sub> magnetic nanocomposite (pH = 3, FeNi<sub>3</sub>/SiO<sub>2</sub> nanocomposite dose = 1 g/L).

Table 1  
Model isotherm constants of Reactive Red 195 adsorption by FeNi<sub>3</sub>/SiO<sub>2</sub> magnetic nanocomposite

Langmuir isotherm			Freundlich isotherm		
R <sup>2</sup>	Q <sub>max</sub> (mg/g)	b (L/mg)	R <sup>2</sup>	N	K <sub>F</sub> (mg/g)
0.999	0.83	34.58	0.902	1.04	0.88

Table 2  
Kinetic parameters of Reactive Red 195 adsorption kinetics with FeNi<sub>3</sub>/SiO<sub>2</sub> magnetic nanocomposites

Pseudo-first-order kinetics			Pseudo-second-order kinetics		
R <sup>2</sup>	q <sub>e</sub> (mg/g)	K <sub>1</sub> (min <sup>-1</sup> )	K <sub>2</sub> (g/mg min)	q <sub>e</sub> (mg/g)	R <sup>2</sup>
0.922	2.8	0.0272	0.026	17.95	0.999

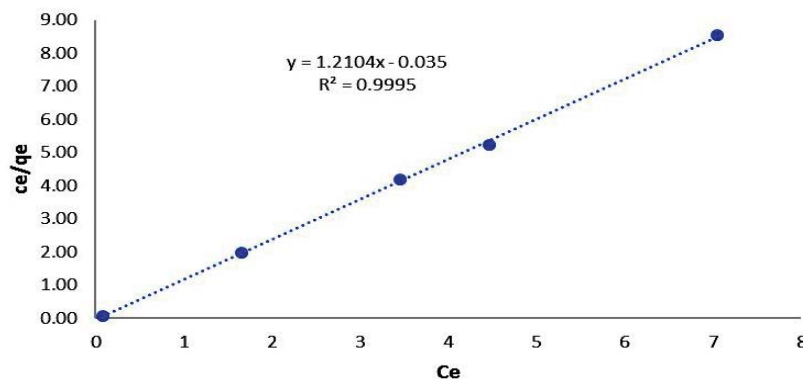


Fig. 4. Langmuir isotherm model on the absorption of Reactive Red 195 dye with FeNi<sub>3</sub>/SiO<sub>2</sub> magnetic nanocomposites.

kinetic model was obtained by plotting  $\ln(q_e - q_t)$  vs.  $t$  and the pseudo-second-order kinetics by  $t/q_t$  against  $t$  (Fig. 5). The pseudo-first-order kinetic graph was used to calculate the coefficient  $R^2$  and the constant value  $K_1$ , and in the pseudo-second-order kinetic diagram, the amount of  $K_2$  and  $q_e$  were obtained from the calculation of the graph slope and width from the origin. In this study, since the  $R^2$  value in pseudo-second-order kinetic was 0.99, it follows the pseudo-second-order model.

### 3.2. Fenton-like catalytic process for Reactive Red 195 dye degradation (FeNi<sub>3</sub>/SiO<sub>2</sub>@H<sub>2</sub>O<sub>2</sub>)

#### 3.2.1. Effect of pH

The effect of pH on the removal of Reactive Red 195 in dye adsorption and catalytic Fenton-like processes are

shown in Fig. 6. The effect of initial pH of solution (3, 5, 7, 9, and 11) on the rate of removal of Reactive Red 195 dye by catalytic Fenton-like process (FeNi<sub>3</sub>/SiO<sub>2</sub>@H<sub>2</sub>O<sub>2</sub>) was investigated and the highest percentage removal at pH = 3 was obtained at 87% and it was found that the removal efficiency decreased with increasing pH. In both Reactive Red 195 dye adsorption and removal processes, the highest efficiency was obtained at pH = 3. As shown in Fig. 9, the highest dye removal efficiency was 85% in the adsorption process and 87% in the dye removal process showing that by adding H<sub>2</sub>O<sub>2</sub> to the process, the Reactive Red 195 dye removal efficiency increased.

In a study by Kamranif et al. [1] on the removal of Reactive Red 195 dye by barberry powder and ash, it was found that at pH = 3 it had the highest adsorption capacity, which decreased with increasing pH value. Also, in a study by Djafarzadeh [32] on the Reactive Red 195 dye

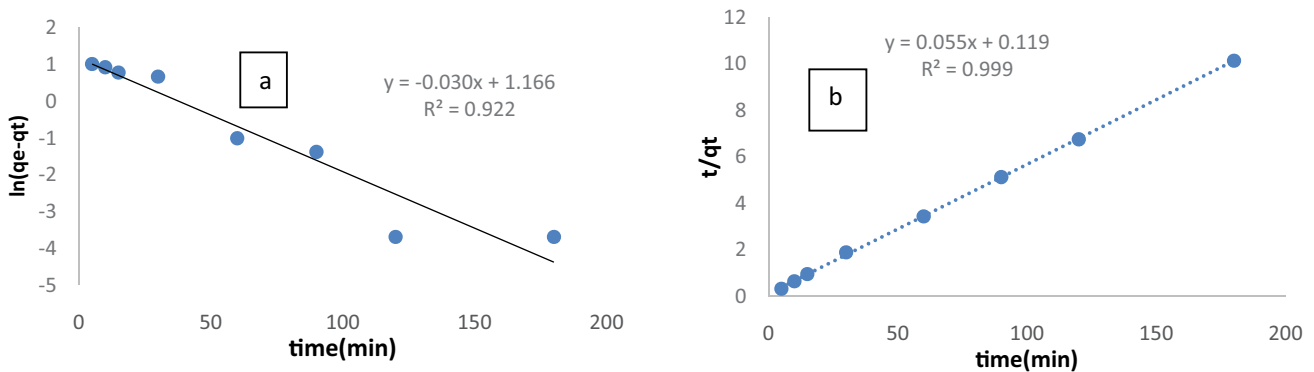


Fig. 5. Pseudo-first-order kinetics (a) and the pseudo-second-order kinetics (b) in Reactive Red 195 dye adsorption process using FeNi<sub>3</sub>/SiO<sub>2</sub>.

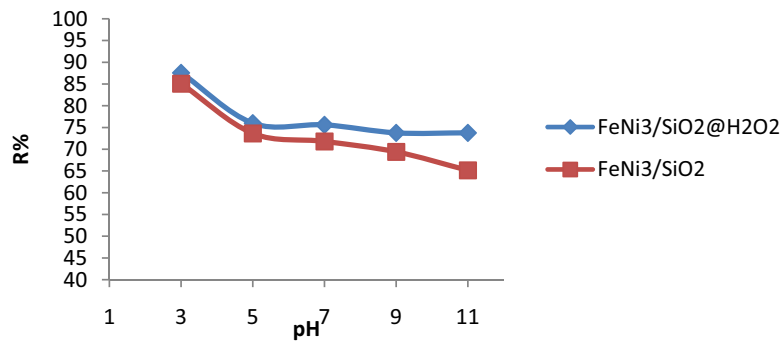
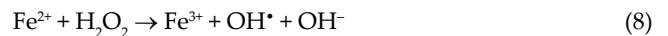


Fig. 6. Effect of the initial pH of the solution on the rate of adsorption and removal of Reactive Red 195 (dose of FeNi<sub>3</sub>/SiO<sub>2</sub> nanocomposite 1 g/L, initial dye concentration 20 mg/L, H<sub>2</sub>O<sub>2</sub> concentration 150 mg/L, and reaction time 60 min).

mineralization by electro-Fenton process, the highest removal percentage was at pH = 3 and about 93% which is in conformity with the present study. As we know, pH is a very important parameter for the production of OH<sup>•</sup> radicals in the Fenton-like and Fenton process. According to the present research, the removal efficiency of Reactive Red 195 was increased at low pH [19]. At pHs above 3, Fe(III) precipitates as Fe(OH)<sub>3</sub> and decomposes H<sub>2</sub>O<sub>2</sub> into water and oxygen, so the formation of Fe(II) complexes at higher pH reduces its concentration in the solution. In contrast, Fe(II)

re-production is prevented by the reaction of Fe<sup>3+</sup> and H<sub>2</sub>O<sub>2</sub> (Eq. (8)) at acidic pH [33]:



### 3.2.2. Effect of the initial concentration of Reactive Red 195

The initial concentration of Reactive Red 195 is effective in removing it from the sample by the catalytic Fenton-like process (FeNi<sub>3</sub>/SiO<sub>2</sub>@H<sub>2</sub>O<sub>2</sub>), and as shown in Fig. 7, the

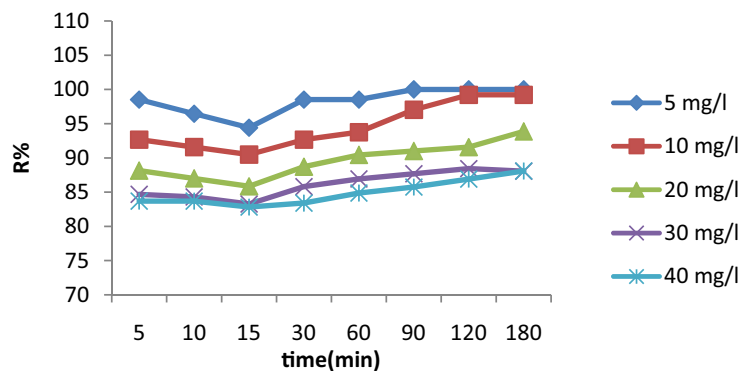


Fig. 7. Effect of the initial dye concentration on the rate of Reactive Red 195 dye removal at different times by the Fenton-like catalytic process (FeNi<sub>3</sub>/SiO<sub>2</sub>@H<sub>2</sub>O<sub>2</sub>) (pH = 3, adsorbent mass = 1 g/L, and concentration H<sub>2</sub>O<sub>2</sub> = 150 mg/L).

removal performance decreases with increasing concentration. At the lowest dye concentration, the removal percentage was 100% and by increasing the dye concentration to 40 mg/L, the removal percentage decreased to 88%.

Also, the results by Bayar and Erdogan [34] on red 45 removals by the Fenton and Fenton-like process showed that with increasing color concentration, the removal efficiency decreased. According to a study by Chladkova et al. [4] revealed that lower concentrations of Reactive Red 195 dye by  $\text{TiO}_2$  nanoparticles increases the removal percentage. The reason is that as the concentration of the color increases, the number of dye molecules increases with any change in the number of  $\text{OH}^\bullet$  radicals. As the  $\text{Fe}^{2+}$  and  $\text{H}_2\text{O}_2$  concentrations are constant, the number of available  $\text{OH}^\bullet$  radicals decrease and as a result, the removal performance decreases with increasing dye concentration [34,35].

### 3.2.3. Effect of initial dose of $\text{FeNi}_3/\text{SiO}_2$ magnetic nanocomposite in the presence of $\text{H}_2\text{O}_2$

In order to determine the effective adsorbent dose, experiments were carried out to explore the effect of nano-composite dosage on the Reactive Red 195 dye removal process by catalytic Fenton-like process ( $\text{FeNi}_3/\text{SiO}_2@/\text{H}_2\text{O}_2$ ). Fig. 8 illustrates the effect of nano-composite dose on dye removal. Based on the results, the highest percentage of removal was obtained at the dose of 4 g/L and

rate of 94% and the lowest percentage in nanocomposites dose of 1 g/L at a rate of 87%.

According to Fig. 8, when the nanocomposite dose increased, the removal efficiency increased, the reason for the diminished removal percentage with the elevation of nanocomposite dose can be attributed with increasing of the number of active adsorption sites on the adsorbent surface and thus increases the efficiency of dye removal [5,36].

In a study by Belessi et al. [30] on the removal of Reactive Red 195 dye by  $\text{TiO}_2$  nanoparticles, the results showed that the highest removal rate was 100% at the highest adsorbent dose of 2 g/L. Similarly, in a study by Farooghi et al. [37] on lead removal from aqueous solution by  $\text{FeNi}_3/\text{SiO}_2$  nanocomposite, results showed that when the adsorbent dose increased, the percentage of pollutant removal increased.

### 3.2.4. Effect of initial concentration of hydrogen peroxide

Addition of hydrogen peroxide to the catalytic Fenton-like process ( $\text{FeNi}_3/\text{SiO}_2@/\text{H}_2\text{O}_2$ ) in most cases increases the amount of catalytic oxidation. In order to maintain its performance, it is necessary to select the  $\text{H}_2\text{O}_2$  concentration according to the type and concentration of the contaminant studied [38].

The effect of  $\text{H}_2\text{O}_2$  concentration on RR195 degradation, showed that an increase in  $\text{H}_2\text{O}_2$  concentration from 50 to 100 mg/L significantly affected the initial rate of dye

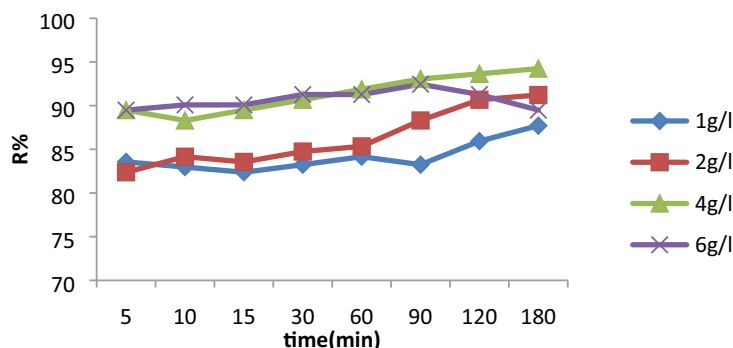


Fig. 8. Effect of the initial dose of  $\text{FeNi}_3/\text{SiO}_2$  nanocomposite on the amount of Reactive Red 195 dye removal at different times (pH = 3, dye concentration = 20 ppm, and  $\text{H}_2\text{O}_2$  concentration = 150 mg/L).

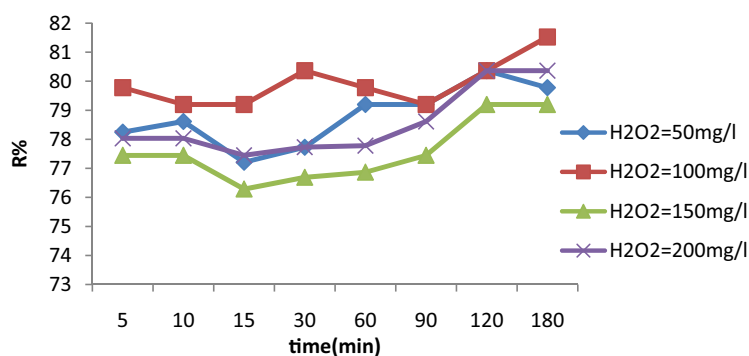
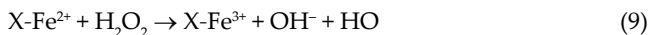


Fig. 9. Effect of the initial concentration of hydrogen peroxide on the amount of RR195 removal at different times (pH = 3, 20 mg/L = dye concentration, and  $\text{FeNi}_3/\text{SiO}_2$  nanocomposite dose = 1 g/L).

removal (Fig. 9). This effect is due to the increase in  $\text{OH}^\cdot$  radicals resulting from the increase in  $\text{H}_2\text{O}_2$  concentration (Eq. (9)), however, with increasing  $\text{H}_2\text{O}_2$  concentration from 150 to 200 mg/L, the dye removal efficiency decreased and the highest removal percentage was obtained at 100 mg/L  $\text{H}_2\text{O}_2$  concentration with the rate was 80%.



The slight decrease in dye removal efficiency of RR195 with increasing  $\text{H}_2\text{O}_2$  concentration may be due to the reaction between  $\text{H}_2\text{O}_2$  and the produced hydroxyl radicals, which results in less active hydroxyl radical

production and is in fact related to the scavenger activity of  $\text{H}_2\text{O}_2$  at high concentrations (Eq. (10)) [19]:



In a study by Wali [13] on the removal of dye and COD from dyeing industry wastewater by Fenton reaction with concentrations of 0.5–6 g/L  $\text{H}_2\text{O}_2$ , the results showed that red 167 dye removal at 3 g/L concentration was 94%, but at higher concentrations, the removal efficiency decreased slightly. Also, in a study by Bayar and Erdogan [34] in the field of Reactive Red 45 dye removal by Fenton and Fenton-like processes, the results showed that the desired dye removal was obtained at concentrations of 100–600 mg/L  $\text{H}_2\text{O}_2$  in which 100–400 mg/L dye removal efficiency increased from 94% to 99% but decreased at concentrations above 400 mg/L.

### 3.2.5. Effect of COD removal on dye removal by Fenton-like method

COD removal in the three phases of pH change, nano-composite dosage change, and Reactive Red 195 concentration change in Fenton-like phase were surveyed and the highest COD removal performance was 41% at pH = 3 and in the RR195 concentration change phase, the highest removal was obtained at 5 mg/L concentration at the rate of 66% and in the nano-composite dose change phase, the highest removal rate was calculated at 6 g/L at the rate of 66% (Fig. 10).

### 3.3. Stability evaluation of $\text{FeNi}_3/\text{SiO}_2$ magnetic nanocomposite

One of the most important advantages of nanoparticles is their recoverability. These nanoparticles can be used several times without significant impact on their efficiency, which is of great economic importance. As shown in Fig. 11a,  $\text{FeNi}_3/\text{SiO}_2$  nanocomposite was used to remove Reactive Red 195 dyes in five cycles, with no significant decrease in efficiency and only about 6% decrease in efficiency. In the first stage of use, the removal percentage was 86%, and in the fifth stage, the removal percentage decreased to 80%. Therefore, the results show that the studied nanocomposite has good stability for dye removal under different conditions and can be reusable. The adsorbent has not been reconstructed, but each time after the dye removal process, it is washed several times with deionized water and re-placed to use [19].

### 3.4. Kinetics of Reactive Red 195 degradation phase in $\text{FeNi}_3/\text{SiO}_2@H_2O_2$ catalytic Fenton process

The pseudo-first-order kinetics was used to investigate the kinetics of the Fenton-like reaction in this study. The  $K_{\text{obs}}$  results at different dye concentrations at 60 min are plotted in Fig. 11b. Accordingly, it is found that as the concentration of color increases, the amount of  $K_{\text{obs}}$  decreases, indicating a decrease in reaction rate with increasing dye concentration [39].

### 3.5. Comparison of $\text{FeNi}_3/\text{SiO}_2@H_2O_2$ with other composites in the degradation of RR195

Comparing the results of this study with other adsorbents is shown in Table 3. Based on these results, it is revealed

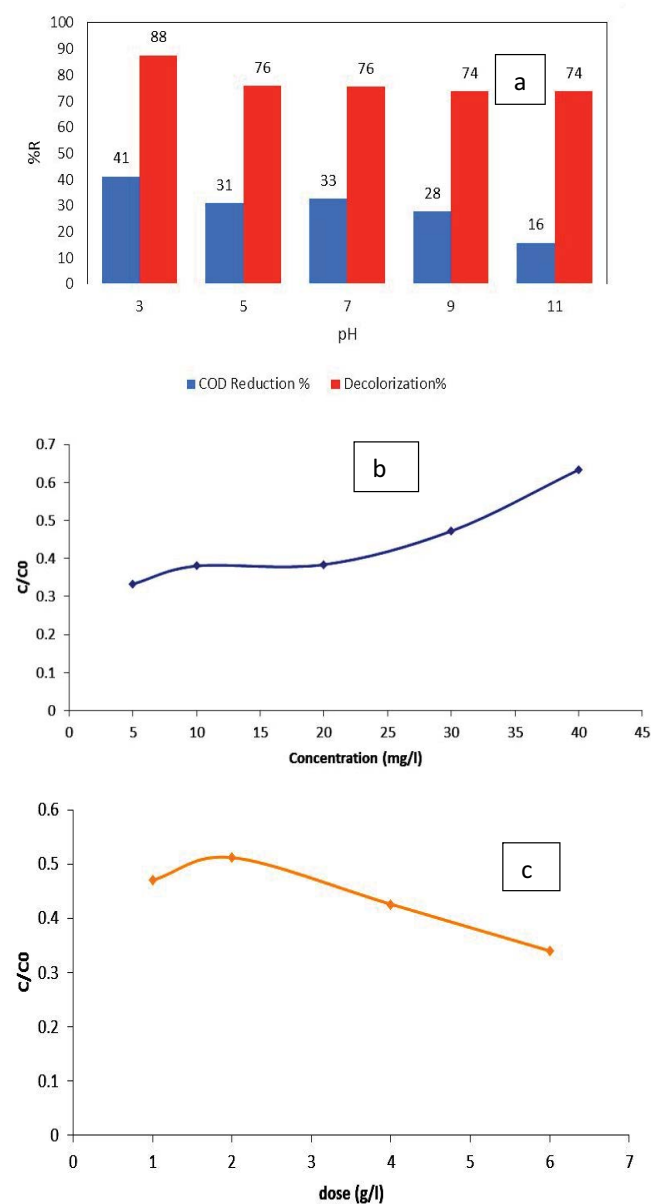


Fig. 10. COD removal efficiency and RR195 dye removal in the phase changes of pH (a), dye concentration changes (b), magnetic nanocomposite dose changes, and (c) in the catalytic Fenton-like process.

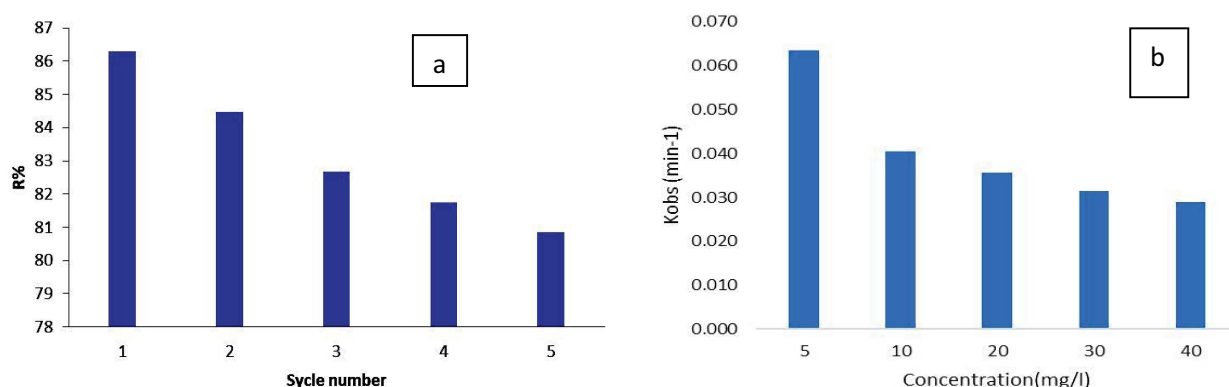
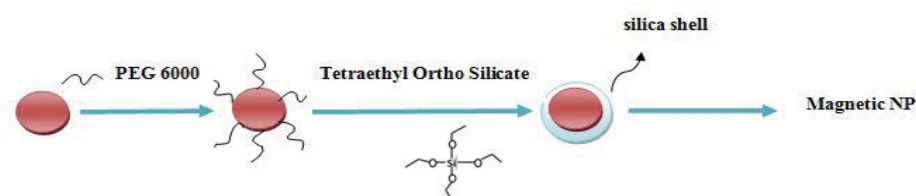


Fig. 11. (a) Stability and reuse of FeNi<sub>3</sub>/SiO<sub>2</sub> magnetic nanocomposite, (b) kinetics graph at different concentrations in the FeNi<sub>3</sub>/SiO<sub>2</sub>@H<sub>2</sub>O<sub>2</sub> process (pH = 3, FeNi<sub>3</sub>/SiO<sub>2</sub> nanocomposite dose = 1 g/L, and H<sub>2</sub>O<sub>2</sub> = 50 mg/L, at time 60 min).



Scheme. 1. Schematic representation of the synthesis of FeNi<sub>3</sub>/SiO<sub>2</sub> magnetic nanocomposite

Table 3

Comparison of FeNi<sub>3</sub>/SiO<sub>2</sub>@H<sub>2</sub>O<sub>2</sub> with other composites in the degradation of RR195

Process	Experimental conditions and results	Reference
Copper cobaltite nanocomposite	Results showed that more than 85% of the 3BF was degraded in 45 min of irradiation	[40]
Fe-ZSM-5@TiO <sub>2</sub>	Results showed that the maximum RR195 dye degradation was obtained at 400 mg/L photo-catalyst, pH = 3, and dye concentration of 50 mg/L	[41]
Magnetic graphene oxide nanocomposite	Highest adsorption capacity of MGO sorbent was obtained at an initial RR195 dye concentration of 325 mg/L, the contact time of 65 min, adsorbent amount of 89.4 mg, and pH of 3	[42]
UV/NaOCl/TiO <sub>2</sub> /Sep	Maximum RR195 removal was 99.9%, respectively, at a dye concentration of 250 mg/L, NaOCl dosage of 50.37 mM, 0.1 g/L weight of TiO <sub>2</sub> /Sep, and pH of 5.45 in 3 h	[43]
CoFe <sub>2</sub> O <sub>4</sub> – ANa nanocomposite	Removal efficiency could be maintained in a wide pH range of 3–6.	[44]
FeNi <sub>3</sub> /SiO <sub>2</sub> @H <sub>2</sub> O <sub>2</sub>	Most removal percentage at pH = 3, initial dye concentration of 5 ppm, adsorbent dose of 6 g/L, and contact time of 90 min were 100%	Present study

that the nanoabsorbent has a very good efficiency in removing Reactive Red 195 dye from aqueous solutions and this is because it has a high surface to volume ratio and in addition, its separation is easier and can be easily separated by an external magnetic field.

#### 4. Conclusion

The results of this study showed that FeNi<sub>3</sub>/SiO<sub>2</sub> magnetic nanocomposite is highly efficient in the process of

catalytic Fenton-like Reactive Red 195 dye removal and is easily separable and reusable due to its high magnetic properties. In this study, the effects of pH, pollutant concentration, adsorbent dose, and contact time were surveyed. At pH = 3, initial dye concentration of 5 ppm, adsorbent dose of 6 g/L, and contact time of 90 min, the highest removal occurred and it was 100%. Therefore, the use of this magnetic nanocomposite in a catalytic Fenton-like process to remove Reactive Red 195 from aqueous media is recommended.

## Acknowledgments

This article is taken from a MSc in Environmental Health Engineering and approved by Birjand University of Medical Sciences. The authors would like to acknowledge the generous support of the university.

## Author contributions

AA performed experiments and write manuscript, BB supervised a whole research project, MK help AA for Fenton-like examination. The manuscript was written with partnership of all authors. All authors have approved the final draft.

## References

- [1] M. Kamranifar, M. Khodadadi, V. Samiei, B. Dehdashti, M.S. Noori, L. Rafati, N. Nasseh, Comparison the removal of Reactive Red 195 dye using powder and ash of barberry stem as a low cost adsorbent from aqueous solutions: isotherm and kinetic study, *J. Mol. Liq.*, 255 (2018) 572–577.
- [2] A. Somayajula, P. Asaithambi, M. Susree, M. Matheswaran, Sono-electrochemical oxidation for decolorization of Reactive Red 195, *Ultrason. Sonochem.*, 19 (2012) 803–811.
- [3] O. Aksakal, H. Uzun, Equilibrium, kinetic and thermodynamic studies of the biosorption of textile dye (Reactive Red 195) onto *Pinus sylvestris* L., *J. Hazard. Mater.*, 181 (2010) 666–672.
- [4] B. Chladkova, E. Evgenidou, L. Kvitek, A. Panacek, R. Zboril, P. Kovar, D. Lambropoulou, Adsorption and photocatalysis of nanocrystalline TiO<sub>2</sub> particles for Reactive Red 195 removal: effect of humic acids, anions and scavengers, *Environ. Sci. Pollut. Res. Int.*, 22 (2015) 16514–16524.
- [5] M.E. Mahmoud, G.M. Nabil, N.M. El-Mallah, H.I. Bassiouny, S. Kumar, T.M. Abdel-Fattah, A dye from water by modified Switchgrass Biochar adsorbent, *J. Ind. Eng. Chem.*, 37 (2016) 156–167.
- [6] M.S. Mate, G. Pathade, Biodegradation of C.I. Reactive Red 195 by *Enterococcus faecalis* strain YZ66, *World J. Microbiol. Biotechnol.*, 28 (2012) 815–826.
- [7] M. Malakootian, M.R. Nabavian, The study of the performance of electrocoagulation in comparison to electro-Fenton processes at decoloration of methylene blue dye from aqueous solutions using iron electrode, *J. Rafsanjan Univ. Med. Sci. Health Serv.*, 14 (2015) 755–768.
- [8] Z. Tahir, S.R. Malik, M. Mehmood, Adsorption studies of Reactive Red 195 dye using modified rice husk, *Sci. Int.*, 28 (2016) 951–954.
- [9] R. Birmole, A. Parkar, K. Aruna, Biodegradation of Reactive Red 195 by a novel strain *Enterococcus casseliflavus* RDB\_4 isolated from textile effluent, *Nat. Environ. Pollut. Technol.*, 18 (2019) 97–109.
- [10] I. Arslan-Alaton, G. Tureli, T. Olmez-Hanci, Treatment of azo dye production wastewaters using photo-Fenton-like advanced oxidation processes: optimization by response surface methodology, *J. Photochem. Photobiol., A*, 202 (2009) 142–153.
- [11] P. Bahmani, A. Maleki, A. Ghahremani, S. Kohzadi, Efficiency of Fenton oxidation process in removal of Remazol Black-B from aqueous medium, *J. Health Hyg.*, 4 (2013) 57–67.
- [12] A.Y. Dursun, O. Tepe, Removal of Chemazol Reactive Red 195 from aqueous solution by dehydrated beet pulp carbon, *J. Hazard. Mater.*, 194 (2011) 303–311.
- [13] F. Wali, Color removal and COD reduction of dyeing bath wastewater by Fenton reaction, *Int. J. Waste Resour.*, 5 (2015) 1–6, doi: 10.4172/2252-5211.1000171.
- [14] N. Daneshvar, V. Vatanpour, A. R. Khataee, M. H. Rasoulifard, S. Rastegar, Decolorization of mixture of dyes containing malachite green and orange II by Fenton-like reagent, *J. Color Sci. Technol.*, 1 (2008) 83–89.
- [15] N.F. Zubair, S. Jamil, H.N. Bhatti, M.A. Shahid, A comprehensive thermodynamic and kinetic study of synthesized rGO-ZrO<sub>2</sub> composite as a photocatalyst and its use as fuel additive, *J. Mol. Struct.*, 1198 (2019) 126869, doi: 10.1016/j.molstruc.2019.07.116.
- [16] N. Nasseh, L. Taghavi, B. Barikbin, M.A. Nasser, Synthesis and characterizations of a novel FeNi<sub>3</sub>/SiO<sub>2</sub>/CuS magnetic nanocomposite for photocatalytic degradation of tetracycline in simulated wastewater, *J. Cleaner Prod.*, 179 (2018) 42–54.
- [17] K.A. Tan, N. Morad, T.T. Teng, I. Norli, P. Panneerselvam, Removal of cationic dye by magnetic nanoparticle (Fe<sub>3</sub>O<sub>4</sub>) impregnated onto activated maize cob powder and kinetic study of dye waste adsorption, *APCBEE Procedia*, 1 (2012) 83–89.
- [18] S. Singh, V.C. Srivastava, T.K. Mandal, I.D. Mall, S.L. Lo, Synthesis and application of green mixed-metal oxide nanocomposite materials from solid waste for dye degradation, *J. Environ. Manage.*, 181 (2016) 146–156.
- [19] C. Yaman, G. Gündüz, A parametric study on the decolorization and mineralization of CI Reactive Red 141 in water by heterogeneous Fenton-like oxidation over FeZSM-5 zeolite, *J. Environ. Health Sci. Eng.*, 13 (2015) 1–12, doi: 10.1186/s40201-015-0162-6.
- [20] H.N. Bhatti, M. Iqbal, A. Nazir, H. Ain, Kinetic study of degradation of basic turquoise blue X-GB and Basic blue X-GRRL using advanced oxidation process, *Z. Phys. Chem.*, 234 (2019) 1803–1817, doi: 10.1515/zpch-2018-1313.
- [21] M. Khodadadi, M.H. Ehrampoush, M.T. Ghaneian, A. Allahresani, A.H. Mahvi, Synthesis and characterizations of FeNi<sub>3</sub>@SiO<sub>2</sub>/TiO<sub>2</sub> nanocomposite and its application in photocatalytic degradation of tetracycline in simulated wastewater, *J. Mol. Liq.*, 255 (2018) 224–232.
- [22] N. Nasseh, T.J. Al-Musawi, M.R. Miri, S. Rodriguez-Couto, A.H. Panahi, A comprehensive study on the application of FeNi<sub>3</sub>@SiO<sub>2</sub>/ZnO magnetic nanocomposites as a novel photo-catalyst for degradation of tamoxifen in the presence of simulated sunlight, *Environ. Pollut.*, 261 (2020) 114127, doi: 10.1016/j.envpol.2020.114127.
- [23] P. Nazari, S.R. Setayesh, Effective degradation of Reactive Red 195 via heterogeneous electro-Fenton treatment: theoretical study and optimization, *Int. J. Environ. Sci. Technol.*, 16 (2019) 6329–6346.
- [24] M. Revathi, B. Kavitha, C. Vedhi, N. Senthil Kumar, Electrochemical detection and quantification of Reactive Red 195 dyes on graphene modified glassy carbon electrode, *J. Environ. Sci. Health, Part C Environ. Carcinog. Ecotoxicol. Rev.*, 37 (2019) 42–54.
- [25] E.W. Rice, R.B. Baird, A.D. Eaton, *Standard Methods for the Examination of Water and Wastewater*, 23rd ed., American Public Health Association, American Water Works Association, Water Environment Federation, 2017, pp. 5–14.
- [26] M. Nasser, S. Sadeghzadeh, A highly active FeNi<sub>3</sub>-SiO<sub>2</sub> magnetic nanoparticles catalyst for the preparation of 4H-benzo [b]pyrans and spirooxindoles under mild conditions, *J. Iran. Chem. Soc.*, 10 (2013) 1047–1056.
- [27] X. Lu, G. Liang, Q. Sun, C. Yang, High-frequency magnetic properties of FeNi<sub>3</sub>-SiO<sub>2</sub> nanocomposite synthesized by a facile chemical method, *J. Alloys Compd.*, 509 (2011) 5079–5083.
- [28] X. Ding, Y. Huang, J. Wang, H. Wu, P. Liu, Excellent electromagnetic wave absorption property of quaternary composites consisting of reduced graphene oxide, polyaniline and FeNi<sub>3</sub>@SiO<sub>2</sub> nanoparticles, *Appl. Surf. Sci.*, 357 (2015) 908–914.
- [29] R. Wang, X. Wang, X. Xi, R. Hu, G. Jiang, Preparation and photocatalytic activity of magnetic Fe<sub>3</sub>O<sub>4</sub>/SiO<sub>2</sub>/TiO<sub>2</sub> composites, *Adv. Mater. Sci. Eng.*, 2012 (2012), doi: 10.1155/2012/409379.
- [30] V. Belessi, G. Romanos, N. Boukos, D. Lambropoulou, C. Trapalis, Removal of Reactive Red 195 from aqueous solutions by adsorption on the surface of TiO<sub>2</sub> nanoparticles, *J. Hazard. Mater.*, 170 (2009) 836–844.
- [31] M. Khodadadi, M.H. Saghi, N.A. Azadi, S. Sadeghi, Adsorption of chromium VI from aqueous solution onto nanoparticle sorbent: Chitozan-Fe-Zr, *J. Mazandaran Univ. Med. Sci.*, 26 (2016) 70–82.
- [32] N. Djafarzadeh, Mineralization of an azo dye Reactive Red 195 by advanced electrochemical electro-Fenton process, *Int. J. Chem.*, 7 (2016) 217–220.
- [33] P. Bautista, A.F. Mohedano, J.A. Casas, J.A. Zazo, J.J. Rodriguez, An overview of the application of Fenton oxidation to industrial

- wastewaters treatment, *J. Chem. Technol. Biotechnol.*, 83 (2008) 1323–1338.
- [34] S. Bayar, M. Erdogan, Removal of COD and color from Reactive Red 195 azo dye wastewater using Fenton and Fenton-like oxidation processes: kinetic studies. *Appl. Ecol. Environ. Res.*, 17 (2019) 1517–1529.
- [35] G. Harichandran, S. Prasad, SonoFenton degradation of an azo dye, Direct Red, *Ultrason. Sonochem.*, 29 (2016) 178–185.
- [36] J. Anwar, U. Shafique, M. Salman, W. Zaman, A. Dar, S. Anwar, Removal of Pb(II) and Cd(II) from water by adsorption on peels of banana, *Bioresour. Technol.*, 101 (2010) 1725–1755.
- [37] A. Farooqhi, M.H. Sayadi, M.R. Rezaei, A. Allahresani, An efficient removal of lead from aqueous solutions using FeNi<sub>3</sub>@SiO<sub>2</sub> magnetic nanocomposite, *Surf. Interfaces*, 10 (2018) 58–64.
- [38] M. Hoseini, G. Safari, H. Kamani, J. Jaafari, A. Mahvi, Survey on removal of tetracycline antibiotic from aqueous solutions by nano-sonochemical process and evaluation of the influencing parameters, *Iran. J. Health Environ.*, 8 (2015) 141–152.
- [39] D. Dimitrakopoulou, I. Rethemiotaki, Z. Frontistis, N.P. Xekoukoulotakis, D. Venieri, D. Mantzavinos, Degradation, mineralization and antibiotic inactivation of amoxicillin by UV-A/TiO<sub>2</sub> photocatalysis, *J. Environ. Manage.*, 98 (2012) 168–174.
- [40] M.H. Habibi, Z. Rezvani, Photocatalytic degradation of an azo textile dye (C.I. Reactive Red 195 (3BF)) in aqueous solution over copper cobaltite nanocomposite coated on glass by Doctor Blade method, *Spectrochim. Acta, Part A*, 147 (2015) 173–177.
- [41] N. Aghajari, Z. Ghasemi, H. Younesi, N. Bahramifar, Synthesis, characterization and photocatalytic application of Ag-doped Fe-ZSM-5@ TiO<sub>2</sub> nanocomposite for degradation of Reactive Red 195 (RR 195) in aqueous environment under sunlight irradiation, *J. Environ. Health Sci. Eng.*, 17 (2019) 219–232.
- [42] Z.M. Khoshhesab, Z. Ayazi, M. Dargahi, Synthesis of magnetic graphene oxide nanocomposite for adsorption removal of Reactive Red 195: modelling and optimizing via central composite design, *Int. J. Nanosci. Nanotechnol.*, 16 (2020) 35–48.
- [43] M.H. Karaoğlu, M. Uğurlu, Studies on UV/NaOCl/TiO<sub>2</sub>/Sep photocatalysed degradation of Reactive Red 195, *J. Hazard. Mater.*, 174 (2010) 864–871.
- [44] R. Jayalakshmi, J. Jeyanthi, Simultaneous removal of binary dye from textile effluent using cobalt ferrite-alginate nanocomposite: performance and mechanism, *Microchem. J.*, 145 (2019) 791–800.